

# Effect of A-TIG Welding Process on the Weld Attributes of Type 304LN and 316LN Stainless Steels

M. Vasudevan

(Submitted August 21, 2015; in revised form September 12, 2016; published online February 3, 2017)

The specific activated flux has been developed for enhancing the penetration performance of TIG welding process for autogenous welding of type 304LN and 316LN stainless steels through systematic study. Initially single-component fluxes were used to study their effect on depth of penetration and tensile properties. Then multi-component activated flux was developed which was found to produce a significant increase in penetration of 10–12 mm in single-pass TIG welding of type 304LN and 316LN stainless steels. The significant improvement in penetration achieved using the activated flux developed in the present work has been attributed to the constriction of the arc and as well as reversal of Marangoni flow in the molten weld pool. The use of activated flux has been found to overcome the variable weld penetration observed in 316LN stainless steel with <50 ppm of sulfur. There was no degradation in the microstructure and mechanical properties of the A-TIG welds compared to that of the welds produced by conventional TIG welding on the contrary the transverse strength properties of the 304LN and 316LN stainless steel welds produced by A-TIG welding exceeded the minimum specified strength values of the base metals. Improvement in toughness values were observed in 316LN stainless steel produced by A-TIG welding due to refinement in the weld microstructure in the region close to the weld center. Thus, activated flux developed in the present work has greater potential for use during the TIG welding of structural components made of type 304LN and 316LN stainless steels.

**Keywords** activated flux, austenitic stainless steels, microstructure and mechanical properties, TIG welding

## 1. Introduction

The principal disadvantages of TIG welding lie in the limited thickness of material which can be welded in a single pass, poor tolerance to some material composition (cast-to-cast variations), and the low productivity. Weld penetration achievable in single-pass TIG welding of stainless steel is limited to 3 mm when using argon as shielding gas. Austenitic stainless steel exhibits variable weld joint penetration during TIG welding due to small differences in chemical composition between heats of material (Ref 1). Hence, the major limitations of TIG welding of austenitic stainless steels are due to the limited thickness of material which can be welded in a single pass, poor tolerance to cast-to-cast variations, and the low productivity.

A variant of the TIG process called A-TIG process developed first by E.O. Paton Institute of Electric Welding, Kiev, has been reported to overcome the principal limitations of TIG, namely its poor penetration and its sensitivity to composition. In this process, a thin coating of activating flux is applied to the surface of the material before welding. Dramatic increase in weld bead penetration of as much as 300% has been reported. The application of the flux has been found to

constrict the arc which increases the current density and arc forces acting on the molten weld pool. As a consequence, the weld penetration depth or the welding speed can be substantially increased compared with conventional TIG welding at the same welding current (Ref 2–5). In particular, lot of research has focused on the A-TIG welding process developed by the E.O. Paton Electric Welding Institute (PWI) (Ref 6). It has been claimed that the A-TIG process can achieve in a single pass a full penetration weld in steels and stainless steels up to 12 mm thickness without using a bevel preparation or filler wire. Furthermore, the weldment mechanical properties and soundness are claimed to be unaffected. Many investigations on the mechanism have been made and the two representative theories are constriction of the arc (Ref 4, 5, 7) and reversal of the Marangoni convection in the weld pool (Ref 1, 8–10).

In austenitic stainless steels, the effect of flux on the weld bead geometry, microstructure, and mechanical properties has been studied by many researchers (Ref 4, 11–14). It was found that single-component fluxes improved penetration up to 5 mm without any degradation in the microstructure and mechanical properties of austenitic stainless steel welds. Huang et al. (Ref 11) have reported that use of flux in 304 stainless steel has reduced the hot cracking susceptibility due to the increase in the retained  $\delta$  ferrite. They also reported that angular distortion of the weldment was decreased due to flux. The mechanical properties (Ref 15–17), residual stresses and distortion (Ref 18, 19), and corrosion resistance (Ref 20) of the weld joints produced by A-TIG welding process have been extensively tested and reported. Improvement in creep-rupture life (Ref 16) and impact toughness have been reported. Significant reduction in residual stresses and distortion (Ref 18) of the stainless steel weld joints has also been reported.

Specific advantages claimed for the activating flux process, compared with the conventional TIG process, include (1)

M. Vasudevan, Advanced Welding Processes and Modelling Section, Materials Technology Division, Indira Gandhi Centre for Atomic Research, Kalpakkam 603 102, India. Contact e-mail: dev@igcar.gov.in.

increasing depth of penetration up to 12-mm-thick stainless steel can be welded in a single pass compared with typically 3 mm with conventional TIG, (2) overcoming the problem of cast-to-cast variation in low sulfur (<0.002%) containing stainless steel, (3) reducing weld shrinkage and distortion, (4) reduction in bevel preparation requirements, (5) decreasing the number of weld passes, (6) shortening of weld times, (7) reduced consumption of welding filler wire, and (8) elimination of back gouging and/or grinding. The composition of the activated flux is seldom reported in the literature and is patent-protected. Therefore, it is very useful to develop specific activated flux for A-TIG welding of type 304LN and 316LN stainless steels.

In the present work, systematic development of activated flux for A-TIG welding of type 304LN and 316LN stainless steels has been carried out. First effect of single-component flux on the depth of penetration and tensile properties were evaluated. Then multi-component flux was developed and that activated flux was evaluated for producing deeper penetration during A-TIG welding of type 304LN and 316LN stainless steels. The quantity of flux required for producing the desired depth of penetration has also been determined. Effect of specific activated flux on the microstructure and mechanical properties of type 304LN and 316LN stainless steels has also been studied.

## 2. Experimental

The single-component activating fluxes selected for study were Cr<sub>2</sub>O<sub>3</sub>, TiO<sub>2</sub>, SiO<sub>2</sub>, Fe<sub>2</sub>O<sub>3</sub>, NaF, and CaF<sub>2</sub>. Initially 316LN stainless steel plates were chosen for the development of activated flux. Table 1 gives the chemical composition of the 304LN and 316LN stainless steels base metals and their weld metals. The dimensions of the plates used include two groups, namely 125 mm (*L*) × 50 mm (*W*) × 3 mm (*H*) and 125 mm (*L*) × 50 mm × 5 mm (*H*). The single-component activating flux was mixed with acetone to make it into a paste form and was applied manually with a brush. Bead-on-plate welds were made using TIG welding system in which the torch was moved at constant speed with all the above fluxes. Then, the welded pieces were machined into standard test specimens for tensile testing of all weld specimens. Balance portion was used for metallographic observations.

Flat tensile specimens shown in Fig. 1 made from all weld samples were tested in an Instron 1100 tensile-testing machine at room temperature (RT) and 823 K. Tensile tests were conducted as per ASTM E8-04. Tensile elongations were measured on the specimen manually after carefully putting the fractured pieces together. For each condition, three samples were tested and the average values were reported.

Multi-component flux was prepared by mixing the single-component fluxes in right proportions. The activated flux

consists of SiO<sub>2</sub> (25-40%), TiO<sub>2</sub> (30-50%), Cr<sub>2</sub>O<sub>3</sub> (10-20%), NiO (5-15%), and CuO (5-15%), and the constituents of the activated flux are dissolved in a solvent like acetone to make it in a paste form. The activated flux formulation has been patented, and the patent has already been granted (Ref 21, 22). Specific experiments were conducted by making bead-on-plate welds to determine the quantity of flux required for producing desired depth of penetration on 7-mm-thick type 316LN stainless steel plates. Before applying the flux, the mixture consisting of various fluxes was dissolved in acetone to make it a paste. The paste was then applied on the plate or joint prior to welding. Bead-on-plate welds were made on 9-mm-thick 304LN SS and 316LN SS plates of dimension 125 mm (*L*) × 50 mm (*W*) × 9 mm (*H*) to study the effect of current on depth of penetration and weld bead width for welds made with and without flux. Square-butt joint A-TIG weld joint was made on 10-mm-thick 304LN stainless steel plates of dimensions 250 mm (*L*) × 125 mm (*W*) × 10 mm (*H*) using the multi-component flux in single-pass welding. Square-butt joint A-TIG weld joint was made on 12-mm-thick 316LN stainless steel plates of dimensions 300 mm (*L*) × 125 mm (*W*) × 12 mm (*H*) using the multi-component flux in single-pass welding. Back-up strip of 3-mm-thick stainless steel plate is used to prevent sagging of the weld bead during A-TIG welding of 10- and 12-mm-thick plates. Multi-pass weld joints on 10-mm-thick 304LN stainless steel and 12-mm-thick 316LN stainless steel with V-groove were made using manual TIG welding with 308L filler wire and 316L filler wire of 1.6 mm diameter, respectively. During welding, 100 A current and 13-14 V voltage were recorded. All the A-TIG weld joints and the multi-pass weld joints of 304LN and 316LN stainless were subjected to x-ray radiographic examination. During the examination, the ASME section III class I specification was followed. Root and side bend tests were carried out in bottom ejecting guided bend test fixture following the procedure described in ASTM E190 to assess the integrity of the weld joints. After the tests, dye-penetrant test was carried out to check for cracks. Tensile tests were carried out at RT and at

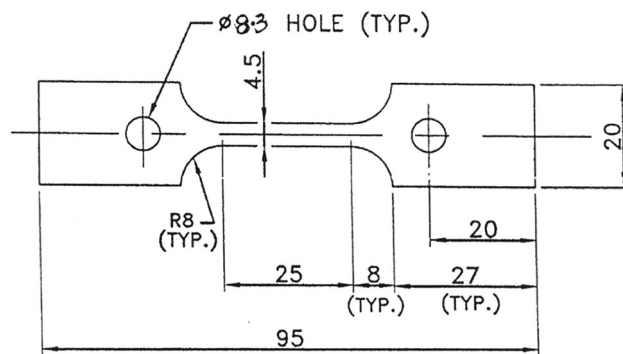


Fig. 1 Flat all weld metal tensile specimen

Table 1 Chemical composition in wt.% of the 304LN and 316LN stainless steel base metals and A-TIG welds

Material	C	Mn	Si	Cr	Ni	Mo	N	S	O	Fe
304LN SS base metal	0.028	1.2	0.8	18.5	10.5	0.05	0.06	0.01	ND	Balance
304LN SS A-TIG weld metal	0.028	1.2	0.8	19	10.2	0.05	0.07	0.014	0.05	Balance
316 LNSS base metal	0.026	1.6	0.5	16.8	12	2.4	0.1	0.005	ND	Balance
316LN SS A-TIG weld metal	0.03	1.5	0.5	17	11.8	2.4	0.09	0.005	0.055	Balance

823 K using cylindrical specimens at a strain rate of  $3.2 \times 10^{-4} \text{ s}^{-1}$  following the procedure described in ASTM E8-04 for small specimen testing. The specimens were made from the pieces cut in the transverse direction to the welded square-butt joint. The specimen dimensions are shown in Fig. 2. Tensile elongations were measured manually after carefully putting the fractured pieces together. Three specimens were tested in all cases and the average values were reported.

Charpy impact tests were carried out on the as welded and as welded and heat-treated conditions. Heat treatment was carried out at 1023 K for 100 h in order to check whether the toughness values meet the specification requirements. Tests were carried out at RT on A-TIG and multi-pass welds using Charpy U notch specimens following the procedure described in ASTM E23. The specimen dimensions are shown in Fig. 3. Three specimens are tested for each case and the average values were reported. Calibrated Fisher Ferritescope was used for measuring the ferrite number on A-TIG welds. In each welded piece, more than ten measurements were made on the weld centerline. Average of those readings was reported. Microstructural examination was carried out using an optical microscope. Samples cut from the welds were polished as per standard metallographic practices and electrolytically etched in 60% nitric acid at 2 V for < 30 s.

### 3. Results and Discussion

#### 3.1 Effect of Single-Component Activated Flux on the Depth of Penetration and Tensile Properties of Type 316 LN Stainless Steel

Systematic development of activated flux involves first evaluating the effect of single-component flux on the weld bead geometry, microstructure and mechanical properties. Figure 4 shows the cross-sections of the weld bead for bead-on-plate TIG weld on 5-mm-thick 316L(N) stainless steel plate made using identical welding parameters without flux and with  $\text{TiO}_2$  flux. Without flux, only partial penetration was achieved for 5-mm-thick plate. It can be seen that the depth of penetration was dramatically increased due to the application of activated flux. With activated flux full penetration was achieved in 5-mm-thick plate at 160 A welding current and 2 mm/s welding speed. Therefore, use of activated flux increased the weld bead penetration and decreased the weld bead width. Table 2 gives the ferrite content measured in 316L(N) base metal, weld metal without flux, and weld metal with different single-component fluxes. The ferrite content was 0 FN in base metal, 0.9 FN in

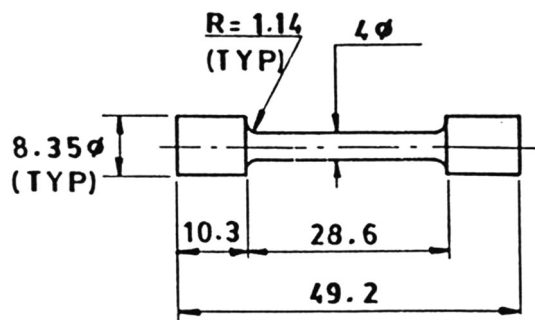


Fig. 2 Transverse weld tensile specimen

weld metal without flux, and in the range of 0.84-1.0 FN in weld metal with different single-component fluxes. The measured ferrite contents in different welds indicated that there were no significant differences between the ferrite content in welds produced without and with flux. Figure 5(a) and (b) shows the typical as solidified microstructures of 5-mm-thick 316LN stainless steel weld produced without and with flux, respectively. The weld metals solidified in Primary austenitic solidification mode. There were also no appreciable differences between the microstructures of the weld metal produced without and with single-component flux.

Figure 6 compares the yield strength (YS), ultimate tensile strength (UTS), and total elongation (TE), at RT and 823 K, for 316L(N) base metal, weld metals produced without and with single-component fluxes for 316LN stainless steel. At RT, the base metal exhibited higher YS compared to the weld metals produced without and with single-component fluxes (Fig. 6a), while the YSs of weld metals produced without and with single-component fluxes were comparable. At 823 K, the YS of the weld metal without flux was slightly higher than that of the base metal and the weld metals produced with single-component fluxes (Fig. 6b). At RT, the UTSs of the base metal and weld metals without and with single-component fluxes were comparable (Fig. 6c). However, at 823 K, the base metal exhibited higher UTS than the weld metals (Fig. 6d), while the UTSs of the weld metals without and with single-component fluxes were comparable except for the weld metal produced with  $\text{Fe}_2\text{O}_3$  which was inferior. At both RT and 823 K, the base metal exhibited better TE than the weld metals (Fig. 6e, f). The TE for the weld metals produced without and with single-component fluxes were comparable except for the weld metal produced with  $\text{Fe}_2\text{O}_3$  which was inferior. The use of single-component flux increased the weld bead penetration, decreased the bead width, and decreased the energy requirement for welding. There was no degradation in the microstructure and mechanical properties of the 316LN stainless steel weld metal produced with flux compared to that of the weld metal without flux. Similar observation that the use of flux has not deteriorated the welding conditions and the microstructure of the welds has been reported for 304 stainless steel (Ref 4). The only apparent disadvantage on using the activated flux was the presence of a thin layer of slag residue on the weld metal surface giving it a rough appearance, which can however be cleaned with a wire brush. If single-component flux only is used, then depth to width ratio obtained is less compared to when multi-component flux is used for the same process parameters. For that reason only multi-component flux is used to achieve enhanced depth of penetration though both fluxes exhibit the same mechanism.

#### 3.2 Development of Multi-component Flux

Based on the results discussed above on the effect of single-component activated flux on penetration, microstructure and mechanical properties, multi-component fluxes were prepared by mixing single-component fluxes in right proportions to achieve enhanced penetration and improved mechanical properties in 304LN and 316LN stainless steels. The compositions of these fluxes were systematically optimized to enhance the penetration for joining thickness up to 10-12 mm in single-pass TIG welding. The constituents of the activated flux are not revealed here as it is patent-protected. It is important that the right quantity of flux need to be applied on the joint area to

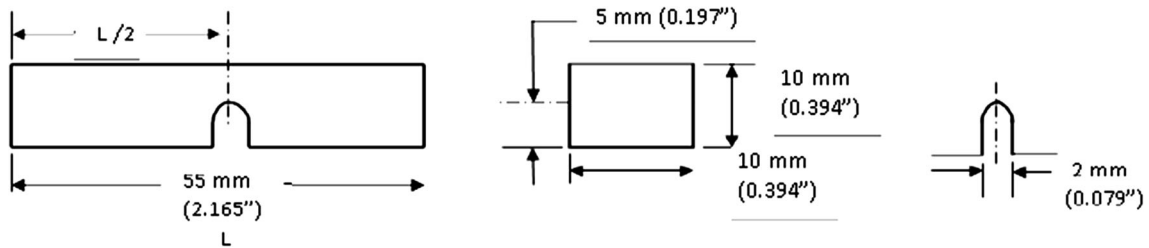


Fig. 3 Charpy impact specimen with U notch

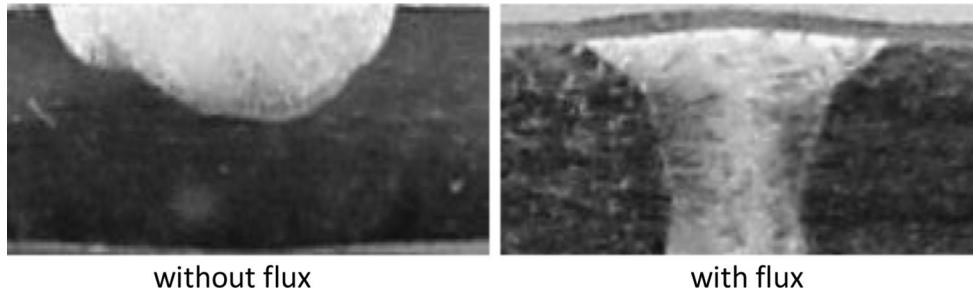


Fig. 4 Comparisons of weld bead cross-sections for 316LN stainless steel bead-on-plate welds metal without and with activated flux for 5-mm-thick plates

Table 2 Ferrite content in base metal and weld metals without and with activated flux

316L(N) SS material	Ferrite number (FN)
Base metal	0 FN
Weld metal without flux	$0.9 \pm 0.07$
Weld metal with $\text{Cr}_2\text{O}_3$	$0.84 \pm 0.1$
Weld metal with $\text{TiO}_2$	$1.0 \pm 0.17$
Weld metal with $\text{SiO}_2$	$0.95 \pm 0.1$
Weld metal with $\text{Fe}_2\text{O}_3$	$0.97 \pm 0.08$
Weld metal with NaF	$1.03 \pm 0.04$
Weld metal with $\text{CaF}_2$	$0.83 \pm 0.1$

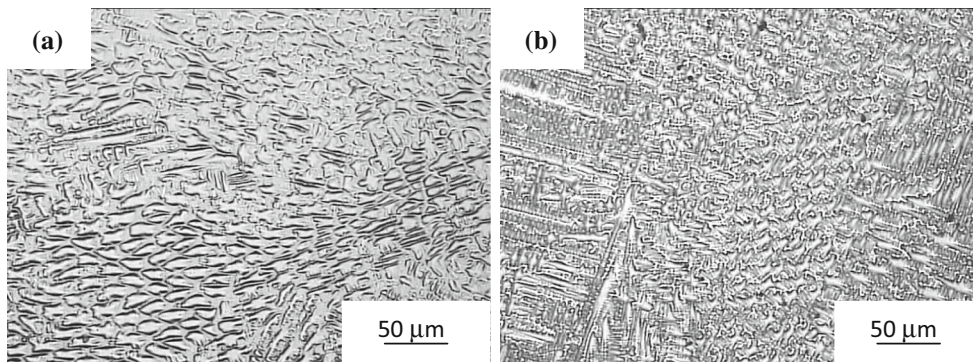
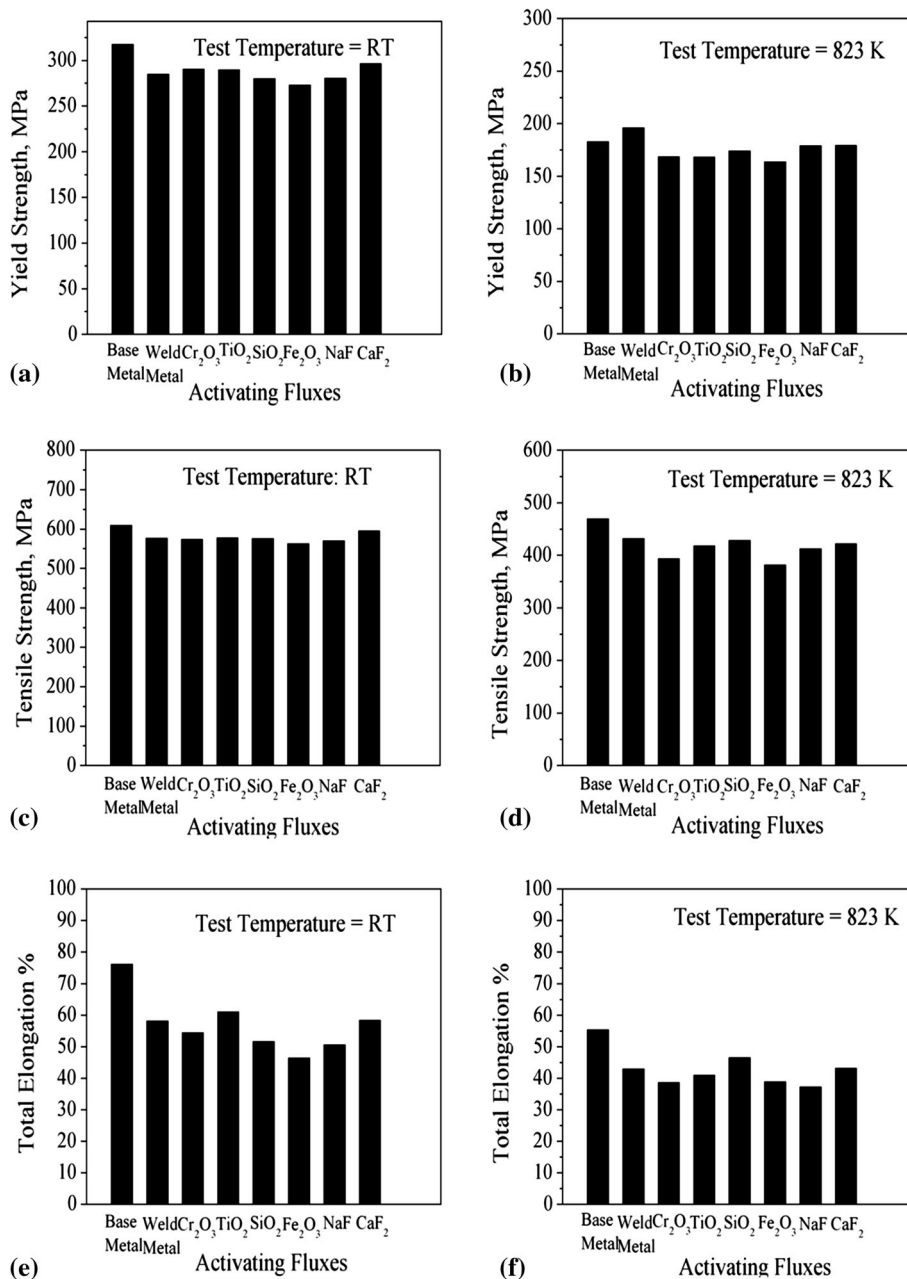


Fig. 5 As solidified microstructures of 316LN stainless steel weld metal: (a) without flux, (b) with flux ( $\text{TiO}_2$ )

achieve the desired depth of penetration is determined. The fluxes were weighed in appropriate amounts for each experiment, and then the paste is made by dissolving in acetone. The entire paste is then uniformly applied on the plate surface prior to welding by using a brush.

Figure 7(a) and (b) shows the quantity of flux required to be applied in terms of the flux density to produce the desired depth of penetration in typical 316LN stainless steel plate. At a flux

density of  $2 \text{ mg/cm}^2$ , full penetration was achieved in 7-mm-thick plate. Beyond that the depth of penetration and bead width values reached saturation. Therefore, the quantity of flux required for welding one meter length of weld using activated flux is approximately 200 mg. Excess quantity of flux used more than 200 mg/m length of weld during welding will only remain as slag residue on the welded surface. Hence, right quantity of flux only needed to be applied on the surface of the



**Fig. 6** Tensile properties of 316LN stainless steel base metal, weld metal without flux and with different single-component fluxes: (a) yield strength at RT, (b), yield strength at 823 K, (c) tensile strength at RT, (d) tensile strength at 823 K, (e) total elongation at RT, (f) total elongation at 823 K

joint prior to welding. The typical variation in depth of penetration as a function of current and torch speed for 316LN stainless steel weld produced by A-TIG welding using multi-component flux is shown in Fig. 8(a) and (b).

The depth of penetration increased with increasing current and decreased with increasing torch speed. At 280 A, depth of penetration of 10 mm could be achieved at 1.33 mm/s torch speed with an arc gap of 1.5 mm. Increase in torch speed decreased the depth of penetration drastically. The effect of variation in welding current on depth of penetration and weld bead width for 304LN and 316LN stainless steels are shown in Fig. 9(a), (b), (c) and (d). The depth of penetration value saturated at 3 mm with increasing current beyond 150 A for 304LN and 316LN stainless steel welds produced without flux.

However, with multi-component flux, depth of penetration increased with increasing current and more than 6 mm depth of penetration could be achieved with a current value of 240 A in single pass. The weld bead width decreased by more than half when produced with flux compared to that of the welds produced without flux. From the Fig. 9(b) the comparison of bead width of TIG and A-TIG welding process on 304LN stainless steel for various current shows that the width has negligible change till 120 A and beyond this current level it has significant variation. The above variation can be explained due to arc constriction. Bead width is decreased in A-TIG welding due to arc constriction. For arc constriction to be effective, the flux needs to be vaporized and the positive ions dissociated from the flux should capture the cooler peripheral electrons in

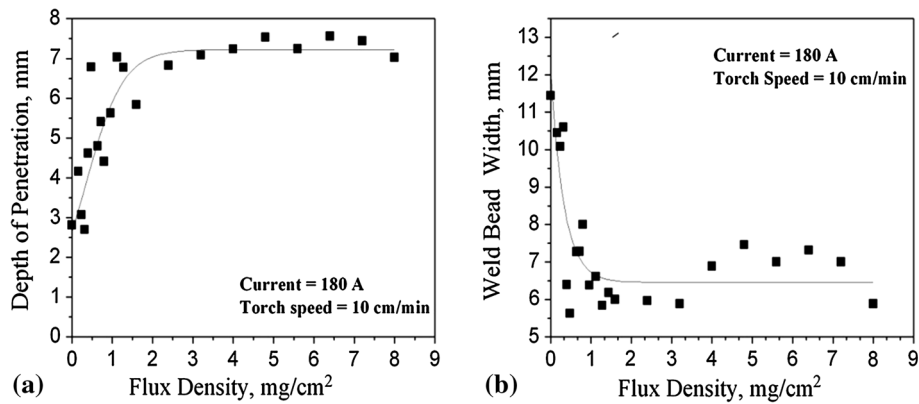


Fig. 7 Effect of quantity of flux on (a) depth of penetration, (b) bead width for 7-mm-thick type 316 LN stainless steel

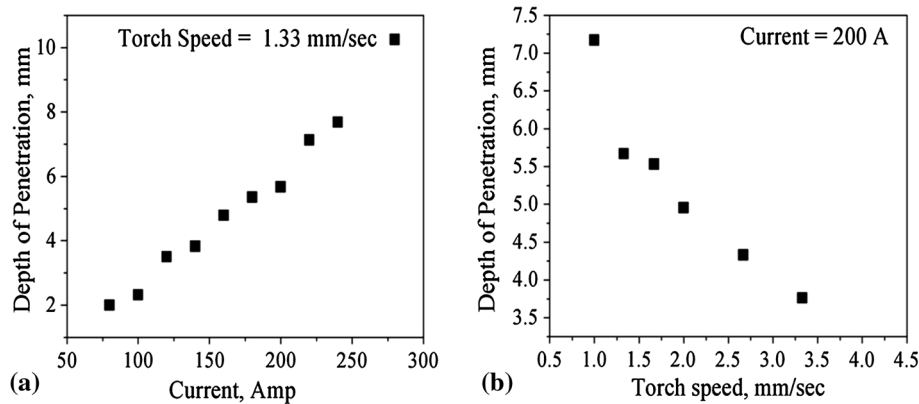


Fig. 8 (a, b) Typical variation in depth of penetration in 316LN stainless steel weld produced by A-TIG welding in single pass as a function of (a) current, (b) torch speed

the ionized plasma of the arc. Therefore, for arc constriction to become very effective, higher current is required. There was an improvement in weld bead profile due to the use of activated flux.

The variable weld penetration, i.e., inconsistency in weld penetration with increasing welding current was observed (Fig. 9c) when the 316LN stainless steel welds were produced without flux. It can be seen from the Fig. 9(c) that the depth of penetration decreased with increasing current when welded without using activated flux. The same welds when produced with activated flux, exhibited consistent variation in the depth of penetration with increasing current. This observation implies that the use of activated flux has mitigated the variable weld penetration caused by low sulfur content in 316LN stainless steel. Similar observation on overcoming the variable weld penetration in 304 stainless steel with low sulfur content using activated flux has been reported (Ref 3). Overcoming the variable weld penetration using activated flux during autogenous TIG welding of austenitic stainless steels was considered as significant achievement.

Figure 10 compares the IR thermal images of the arc column in conventional TIG and A-TIG welds. Decrease in the arc column diameter due to flux was clearly visible. Also, the arc constriction was evident from the decrease in weld bead width observed in A-TIG welds by nearly half the value compared to that of conventional TIG welds. There was no significant difference found in the chemical composition

between the base metal and A-TIG weld metals for both 304LN SS and 316LN stainless steels except for oxygen pick up of approximately 500 ppm in the weld metal as given in Table 1. The base metal oxygen content was not determined in the present work. The 500 ppm of oxygen found in the A-TIG welds should have come from the activated flux. The presence of 500 ppm of oxygen in the weld pool would influence the fluid flow by changing the temperature coefficient of surface tension to a positive value. This would cause the molten metal to flow inward and lead to an increased depth of penetration. This kind of fluid flow behavior is often described as reversal of Marangoni flow (Ref 8). Presence of reversal of Marangoni flow during A-TIG welding has been predicted by a three dimensional mathematical model developed to simulate the weld pool development in a moving A-TIG weld pool with different oxygen and sulfur concentrations (Ref 23). It was shown that critical oxygen content of 280 ppm is required to change the temperature coefficient of surface tension to a positive value in the weld pool. The positive temperature coefficient of surface tension then dominates and controls the fluid flow during A-TIG welding. The further increase in oxygen content would result in inappreciable difference in the weld pool size and shape. If the oxygen content is below 280 ppm, positive and negative coefficients of surface tension coexist in the weld pool and therefore the resultant weld pool may not be deep. The significant enhancement in penetration achieved due to the application of activated flux in the present

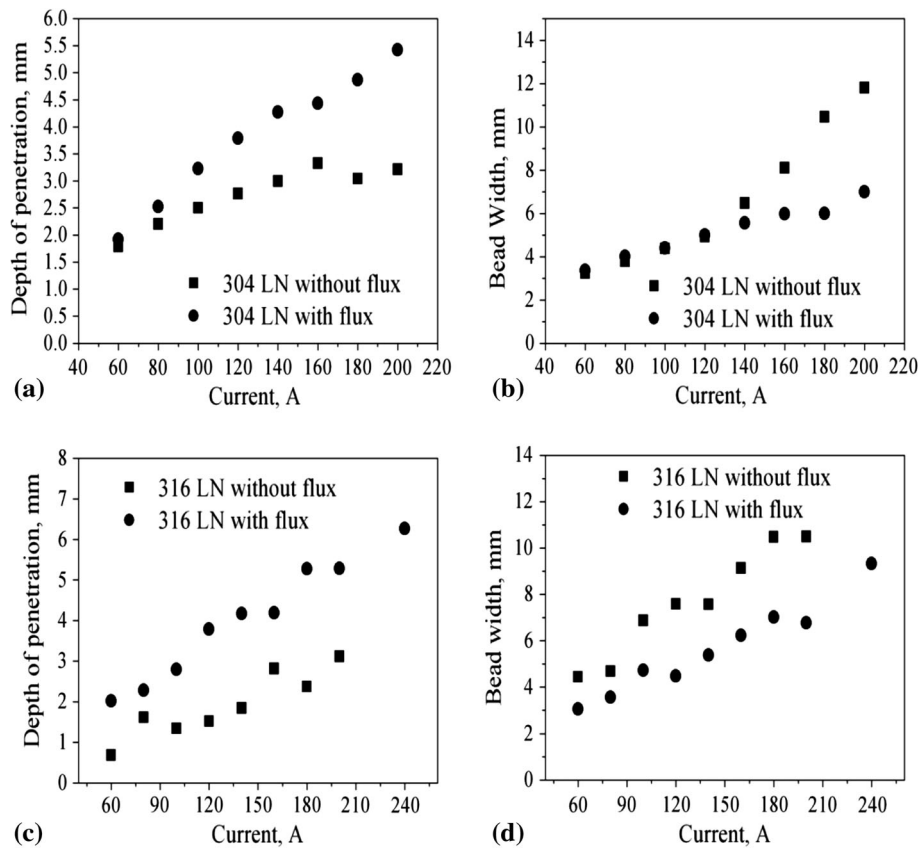


Fig. 9 Effect of activated flux on depth of penetration and weld bead width for 304LN and 316LN stainless steels

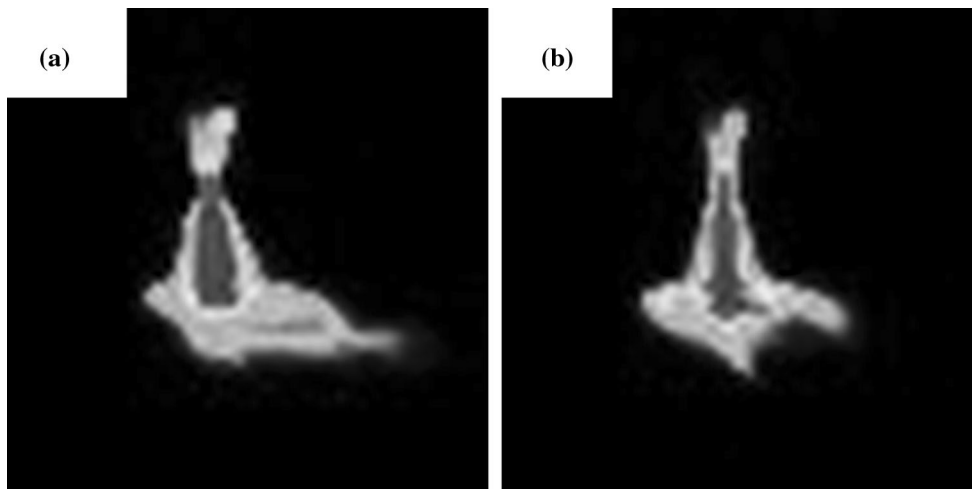


Fig. 10 Infrared thermal images of the arc column for (a) TIG, (b) A-TIG welding

work has been attributed to arc constriction as well as reversal of Marangoni flow caused by dissolved oxygen content in the weld.

### 3.3 Comparison of 304LN (10-mm-Thick) Stainless Steel Weld Joints Made by TIG and A-TIG Welding Processes

Full penetration has been achieved in 10-mm-thick 304LN stainless steel produced by A-TIG welding at a current value of

280 A and a torch speed of 1 mm/s with 1.5 mm arc gap. The weld bead width obtained was narrow with respect to the current used for welding. This indicated that arc constriction was very effective. Back-up strip which provided the support for the molten weld pool from sagging has been machined out to reveal the complete fusion achieved at the root side. The A-TIG weld had passed the radiographic examination. Root-bend- and side-bend-tested specimens in which no defects were observed either by visual examination or by dye-penetrant test

is shown in Fig. 11(a) and (b), respectively. Figure 12(a) and (b) shows the cross-sections of the 304LN stainless steel welds produced by A-TIG and multi-pass welding. It shows complete penetration for the joint thickness of 10 mm. The average value of the ferrite number measured on the weld centerline was 3.4 FN. The as solidified microstructure exhibited primary ferritic solidification mode (Fig. 13a). Multi-pass weld on 10-mm-thick 304LN stainless plates with V-groove was produced using conventional TIG welding with 308L filler wire. Seven passes were required to complete the weld joint. The weld passed radiographic examination and root bend tests without any

indications. The average value of the ferrite content measured on the weld centerline was 10.2 FN. The as solidified microstructure exhibited primary ferritic solidification mode (Fig. 13b). The 304LN stainless steel welds produced by A-TIG welding and multi-pass welding exhibited primary ferritic solidification mode.

Figure 14 compares the variation of hardness as a function of distance from weld centerline for 304LN stainless steel A-TIG and multi-pass weld joints. Hardness values were lower for A-TIG weld as the current used for production of the weld was higher compared to multi-pass weld. There was not much

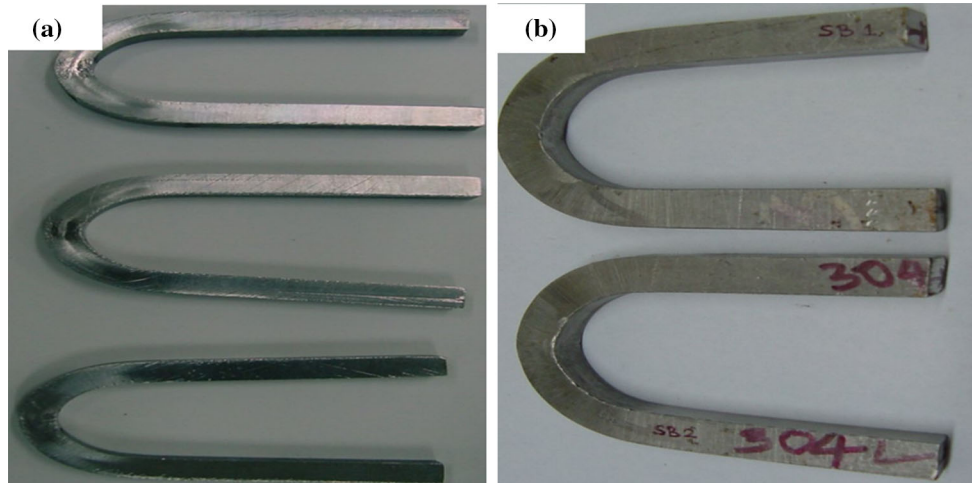


**Fig. 11** (a) Root-bend-tested specimen, (b) side-bend-tested specimens of 304LN stainless steel welds produced by A-TIG welding

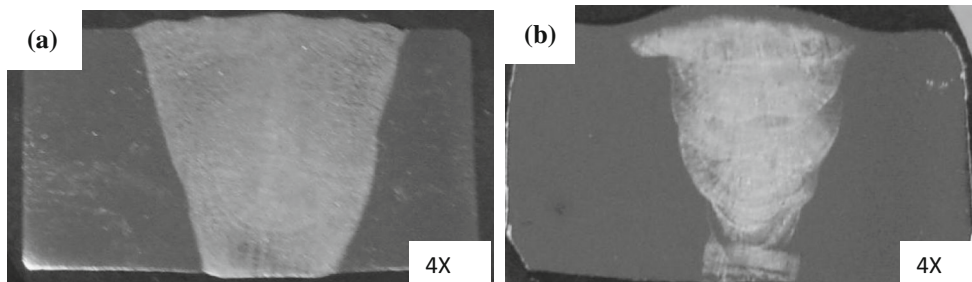


**Fig. 12** Cross-sections of the 304LN stainless steel weld (10 mm thick) produced by (a) A-TIG welding, (b) multi-pass TIG welding

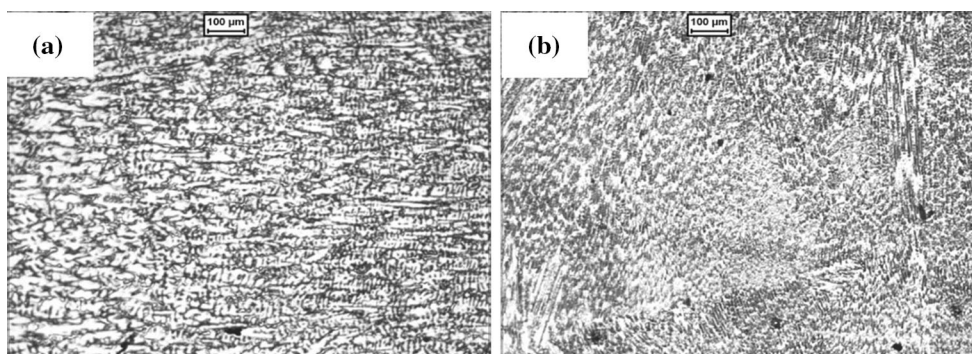


**Fig. 13** Comparison of microstructures of 304LN stainless steel weld (10 mm thick) produced by (a) A-TIG welding, (b) Multi-pass welding



variation in the hardness across the A-TIG weld joint. Table 3 compares the tensile property values for the base metal, conventional TIG weld, and the A-TIG weld joints. The strength and ductility values were higher for the multi-pass

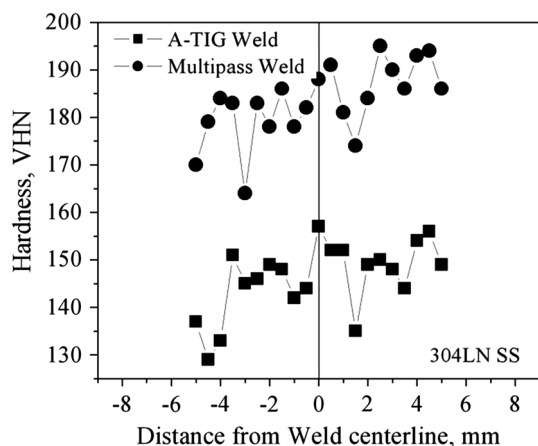


**Fig. 14** Comparison of hardness variation as a function of distance from weld centerline for A-TIG and Conventional TIG welds of 304LN stainless steel

**Table 3** Tensile properties of 304LN base metal, A-TIG weld and the multi-pass weld

Material	0.2% yield strength, Mpa	Tensile strength, MPa	%total elongation
304LN base metal	205	515	40
304LN A-TIG weld	286 ± 4	528 ± 2	36 ± 2
304LN multi-pass weld	379 ± 4	621 ± 3	38 ± 1

**Table 4** Comparison of Impact toughness values between conventional TIG and A-TIG welds on 304LN stainless steel sub-size samples

Material	Impact toughness, J
304LN SS A-TIG weld	70 ± 4
304LN SS multi-pass weld	80 ± 3

weld joint compared to that of the A-TIG weld joint. This could be due to higher ferrite content and low grain size in the multi-pass weld joint compared to A-TIG weld joint. The TE values were comparable between the base and weld metals and there was no degradation in the ductility value compared to that of the base metal. The impact toughness values were slightly higher for multi-pass weld compared to A-TIG weld which is given Table 4. This was attributed to coarser grain size in the weld metal of A-TIG weld joint by 1.2-1.5 times. When full size samples with 10 × 10 mm cross-section was tested, A-TIG weld joint of type 304 LN stainless steel exhibited an average impact toughness of 139 J. The above value is lower than that of the base metal due to the presence of δ-ferrite in the weld metal.

### 3.4 Comparison of 316LN (12-mm-thick) Stainless Steel Welds Made by Conventional Multi-pass TIG Welding and A-TIG Welding Processes

Full penetration has been achieved in 12-mm-thick 316LN stainless steel at a current value of 300 A and torch speed of 1 mm/s with an arc gap of 1.5 mm. The weld joint passed radiographic examination. Root-bend- and side-bend-tested specimens in which no defects were observed either by visual examination or by dye-penetrant test is shown in Fig. 15(a) and (b). The cross-sections of the 316LN stainless steel welds produced by A-TIG and multi-pass welding is shown in Fig. 16(a) and (b). It shows complete penetration for joining thickness of 12 mm produced by A-TIG welding. The Ferrite Number measured on the weld centerline was 2.2 FN. The weld solidified under primary austenitic solidification mode (Fig. 17a). The multi-pass weld joint on 316LN stainless steel was produced using 316L filler wire. Ten passes were required to complete the joint. The weld passed radiographic examination and bend tests without any defect indication. The average value of the ferrite content measured on the weld centerline was 6.2 FN. 316LN stainless steel welds produced by A-TIG welding and multi-pass welding exhibited primary austenitic solidification mode (Fig. 17a, b). Figure 18 compares the hardness variation as a function of distance from weld centerline for A-TIG and conventional TIG weld joints of 316LN stainless steel. Hardness values were lower for the A-TIG weld due to coarser grain size caused by higher peak temperature during A-TIG welding process. There was not much variation in the hardness across

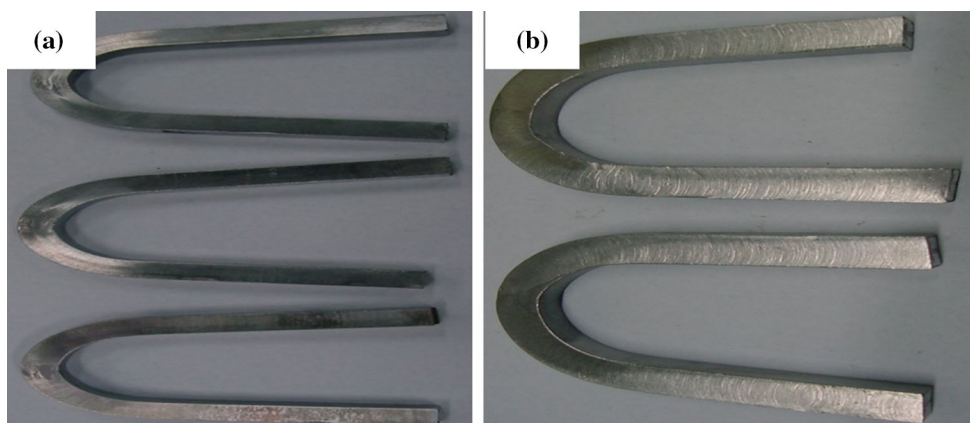


**Fig. 15** (a) Root-bend-tested specimen, (b) side-bend-tested specimens of 316LN stainless steel welds produced by A-TIG welding

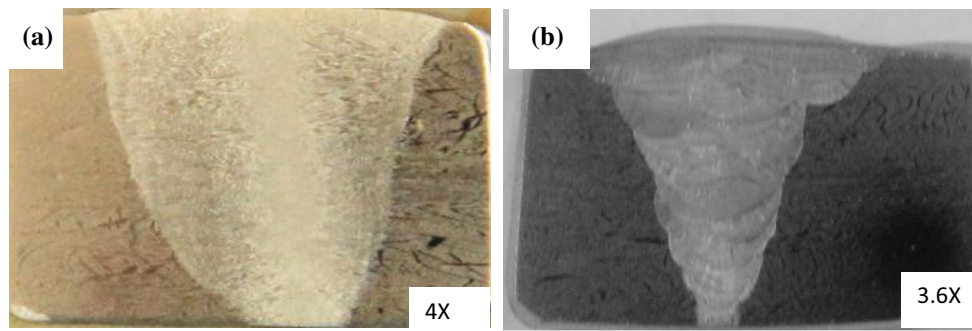


**Fig. 16** Cross-section of the 316 LN Stainless steel weld (12 mm thick) produced by (a) A-TIG welding, (b) Multi-pass TIG welding

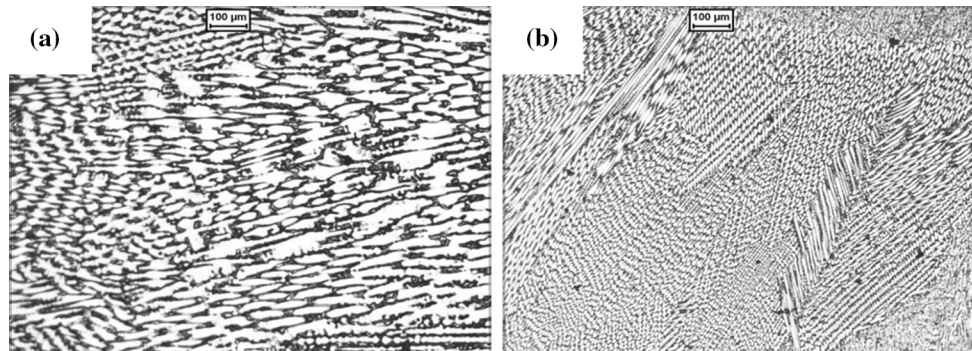


**Fig. 17** Comparison of microstructures of 316LN stainless steel weld metal (12 mm thick) produced by (a) A-TIG welding, (b) Multi-pass welding

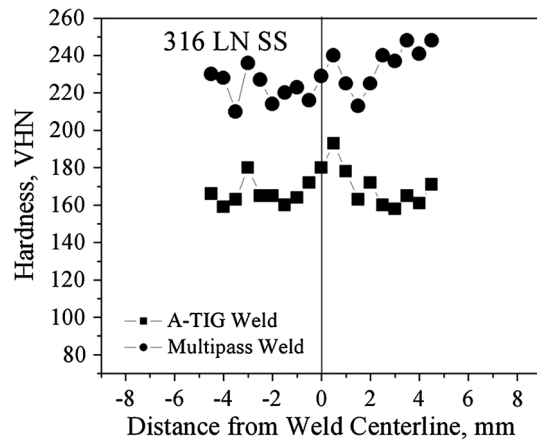


**Fig. 18** Comparison of hardness variation as a function of distance from weld centerline for A-TIG and conventional TIG weld joints of 316LN stainless steel

the A-TIG weld joint. The Comparison of the tensile properties are given in Table 5 which show that the multi-pass weld on 316LN stainless steel exhibited higher strength properties than the A-TIG weld while the ductility values were comparable. High strength properties in multi-pass weld was mainly attributed to the higher ferrite content in the multi-pass weld compared to the A-TIG weld. Impact toughness values were compared between A-TIG and multi-pass weld joints in Table 6. A-TIG weld joint exhibited

**Table 5** Comparison of tensile properties of 316LN stainless steel Base metal, A-TIG weld and multi-pass weld joints

Material	0.2% yield strength, MPa	Ultimate tensile strength, MPa	%total elongation
316LN base metal	205	515	40
316LN A-TIG weld	327 ± 2	578 ± 3	27 ± 1
316LN multi-pass weld	438 ± 2	644 ± 1	25 ± 3

higher impact toughness values. Full size samples of A-TIG weld joint exhibited an average impact toughness value of 250 J. 316LN stainless steel welds produced by A-TIG welding exhibited higher impact toughness values compared to multi-pass welds. This was attributed to some refinement observed in the microstructure at the centre of the weld cross-section as shown in Fig. 19. The refinement of the microstructure in the region close to the weld centre probably was caused by formation of two or three vortices that have different positions, strength and directions as claimed by Zhao et al. (Ref 23) based on the 3D mathematical model. Similarly, Rodriguez et al. (Ref 12), reported the occurrence of some refinement of microstructure in 304 stainless steels welds produced by A-TIG welding. The impact toughness value of the 316LN stainless steel weld produced by A-TIG welding in the heat-treated condition exceeded the minimum specified toughness of the austenitic stainless steel weld (3 dj/cm<sup>2</sup>) in the heat-treated condition.

**Table 6 Comparison of impact toughness values for A-TIG weld joint with multi-pass weld joint for type 316LN stainless steels on sub-size samples**

Material and condition	Impact toughness, J	Impact strength, dj/cm <sup>2</sup>
316LN A-TIG welds	111 ± 3	22
316LN multi-pass welds	77 ± 5	15.4
316LN A-TIG welds + PWHT 1023 K + 100 h	24 ± 2	4.8
316LN multi-pass weld + PWHT 1023 K + 100 h	17 ± 3	3.4

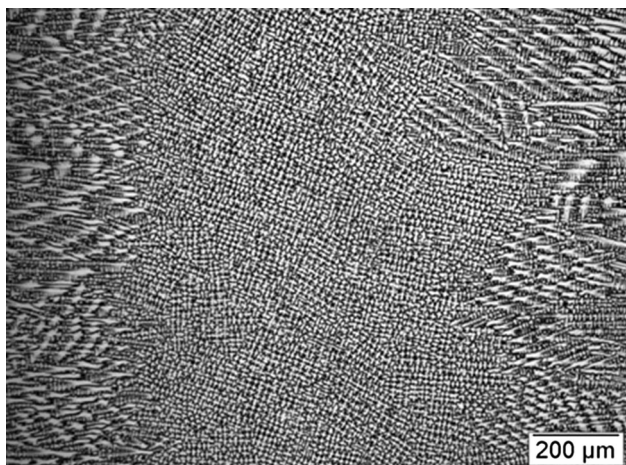


**Fig. 19** Microstructure of the 316LN stainless steel A-TIG weld

## 4. Conclusions

1. The specific activated flux has been developed in the present work for enhancing the penetration during autogenous TIG welding of 304LN and 316LN stainless steels through systematic study. The use of activated flux produced a significant increase in penetration of 10-12 mm in single-pass TIG welding of 304LN and 316LN stainless steels.
2. The significant improvement in penetration achieved using the activated flux developed in the present work was attributed to the constriction of the arc and as well as reversal of Marangoni flow in the molten weld pool. The dissolved oxygen content of 500 ppm in the weld from the flux would change the temperature coefficient of surface tension to a positive value and lead to reversal of Marangoni flow in the weld pool. So, combined operation of the above two mechanisms only lead to increased penetration by as much as 300% in 304LN and 316LN stainless steels produced by A-TIG welding.
3. The use of activated flux has been found to overcome the variable weld penetration observed in 316LN stainless steel with <50 ppm of sulfur.
4. The A-TIG welds produced in the present work were sound and passed radiographic examination and bend tests without any indications. There was residual fused flux layer produced on the face of the A-TIG welds that had to be removed using wire brush. The use of activated flux was found not to cause any significant change in the chemical composition of the weld metals compared to that of the base metals.
5. The average measured ferrite content of the 304LN (10-mm-thick) and 316LN (12-mm-thick) stainless steel weld joints produced by A-TIG welding were 3.4 and 2.2

respectively. The 304LN stainless steel weld produced by A-TIG welding solidified in primary ferritic solidification mode while the 316LN stainless steel weld produced by A-TIG welding solidified in primary austenitic solidification mode.

6. The transverse strength properties of the 304LN and 316LN stainless steel weld joints produced by A-TIG welding exceeded the minimum specified strength values of the base metals. Improvement in toughness values were observed in 316LN stainless steel weld produced by A-TIG welding due to some refinement in the weld microstructure in the region close to the weld center caused by convection currents.
7. There was no degradation in the microstructure and mechanical properties of the A-TIG weld joints compared to that of the weld joints produced by conventional TIG welding. So activated flux developed in the present work has greater potential for use during the welding of structural components made of 304LN and 316LN stainless steels.

## References

1. K.C. Mills and B.J. Keene, Factors Affecting Variable Penetration, *Int. Mater. Rev.*, 1990, **35**(4), p 185–216
2. W. Lucas and D.S. Howse, Activating Flux—Increasing the Performance and Productivity of the TIG and Plasma Processes, *Weld. Met. Fabr.*, 1996, **64**(1), p 11–17
3. T. Paskell, C. Lundin, and H. Castner, GTAW Flux Increases Weld Joint Penetration, *Weld. J.*, 1997, **76**(4), p 57–62
4. P.J. Modenesi, E.R. Apolinario, and I.M. Pereira, TIG Welding with Single-Component Fluxes, *J. Mater. Process. Technol.*, 2000, **99**(1–3), p 260–265
5. M. Tanaka, T. Shimizu, H. Terasaki, M. Ushio, C.L. Koshiishi, and C.L. Yang, Effects of Activating Flux on Arc Phenomena in Gas Tungsten Arc Welding, *Sci. Technol. Weld. Join.*, 2000, **5**(6), p 397–402
6. P.C.J. Anderson and R. Wiktorowicz, Improving productivity with A-TIG welding, *Weld. Met. Fabr.*, 1996, **64**(3), p 108–109
7. D. Fan, R. Zhang, Y. Gu, and M. Ushio, Effect of Flux on A-TIG Welding of Mild Steels, *Trans. JWRI*, 2001, **30**, p 35–40
8. C.R. Heiple and J.R. Roper, Mechanism for Minor Element Effect on GTA Fusion Zone Geometry, *Weld. J.*, 1982, **61**(4), p 97s–102s
9. S.W. Pierce, P. Burgardt, and D.L. Olson, Thermocapillary and Arc Phenomena in Stainless Steel Welding, *Weld. J.*, 1999, **78**(2), p 45s–52s
10. S. Lu, H. Fujii, H. Sugiyama, and K. Nogi, Mechanism and Optimisation of Oxide Fluxes For Deep Penetration in Gas Tungsten Arc Welding, *Metall. Mater. Trans. A*, 2003, **34A**, p 1901–1907
11. H.Y. Huang, S.W. Shyu, K.H. Tseng, and C.P. Chou, Evaluation of TIG Flux Welding on the Characteristics of Stainless Steel, *Sci. Technol. Weld. Join.*, 2005, **10**(5), p 566–573
12. A. Rodrigues and A. Loureiro, Effect of Shielding Gas and Activating Flux on Weld Bead Geometry in Tungsten Inert Gas Welding of Austenitic Stainless Steel, *Sci. Technol. Weld. Join.*, 2005, **10**(6), p 760–765

13. S. Leconte, P. Paillard, and J. Saindrenan, Effect of Fluxes Containing Oxides on Tungsten Inert Gas Welding Process, *Sci. Technol. Weld. Join.*, 2006, **11**(1), p 43–47
14. L. Sanbao, Y. Chunli, L. Fengyao, W. Lin, and S. Sheng, Effect of Activating Fluxes on Weld Mechanical Properties in TIG Welding, *China Weld.*, 2001, **10**(2), p 46–50
15. M. Vasudevan, *Computational and Experimental Studies on Arc Welded Stainless Steels*. Ph.D. Thesis, Indian Institute of Technology, Madras, Chennai, 2007
16. T. Sakthivel, M. Vasudevan, K. Laha, P. Parameswaran, K.S. Chandravathi, M.D. Mathew, and A.K. Bhaduri, Effect of Welding Processes on the Creep Rupture Behaviour of type 316LN Stainless Steel Weld Joints, *Mater. Sci. Eng. A*, 2011, **528**(22–23), p 6971–6980
17. V. Maduraimuthu, M. Vasudevan, V. Muthupondi, A.K. Bhaduri, and T. Jayakumar, Study of the Effect of Activated Flux on the Microstructure and Mechanical Properties of Mod. 9Cr–1Mo steel, *Metall. Mater. Trans. B*, 2012, **43**(1), p 123–132
18. P. Palanichamy, M. Vasudevan, and T. Jayakumar, Measurement of Residual Stresses in Austenitic Stainless Steel Weld Joints Using an Ultrasonic technique, *Sci. Technol. Weld. Join.*, 2009, **14**(2), p 166–171
19. P. Vasantharaja, V. Maduraimuthu, M. Vasudevan, and P. Palanichamy, Measurement of Residual Stresses in Austenitic Stainless Steel Weld Joints Using an Ultrasonic Technique, *Mater. Manuf. Process.*, 2012, **27**(12), p 1376–1381
20. A. Ravishankar, S. Niyanth, M. Vasudevan, and K. Mudali, Microstructural Characterization and Corrosion behaviour of type 304 L Stainless Steel TIG weld joints in Nitric Acid, *Corrosion*, 2012, **68**(8), p 762–773
21. M. Vasudevan, A.K. Bhaduri, and B. Raj, *A Penetration Enhancing Flux Formulation For Tungsten Inert Gas (TIG) Welding of Austenitic Stainless Steel and Its Application*. United States Patent No. 8097826 B2, 17 Jan 2012
22. M. Vasudevan, A.K. Bhaduri, and B. Raj, *A Penetration Enhancing Flux Formulation for Tungsten Inert Gas (TIG) Welding of Austenitic Stainless Steel and Its Application*. United Kingdom Patent No. GB 2446905 B, 16 Feb 2011
23. Y. Zhao, H. Zhou, and Y. Shi, The Study of Surface Active Element on Weld Pool Development in A-TIG Welding, *Model. Simul. Mater. Sci. Eng.*, 2006, **14**, p 331–349